

Tyrosine kinase receptor Axl enhances entry of *Zaire ebolavirus* without direct interactions with the viral glycoprotein

Melinda A. Brindley ^{a,1,2}, Catherine L. Hunt ^{a,2}, Andrew S. Kondratowicz ^a, Jill Bowman ^a, Patrick L. Sinn ^b, Paul B. McCray Jr. ^b, Kathrina Quinn ^c, Melodie L. Weller ^c, John A. Chiorini ^c, Wendy Maury ^{a,*}

^a Department of Microbiology, University of Iowa, Iowa City, IA 52242, USA

^b Department of Pediatrics, University of Iowa, Iowa City, IA 52242, USA

^c Molecular Physiology and Therapeutics Branch, National Dental and Craniofacial Research Branch, National Institutes of Health, Bethesda, MD 20892, USA

ARTICLE INFO

Article history:

Received 29 December 2010
Returned to author for revision
28 January 2011
Accepted 4 April 2011
Available online 6 May 2011

Keywords:

Axl
Filovirus
Ebolavirus
Marburgvirus
Virus entry
Tyrosine kinase receptors

ABSTRACT

In a bioinformatics-based screen for cellular genes that enhance *Zaire ebolavirus* (ZEBOV) transduction, *AXL* mRNA expression strongly correlated with ZEBOV infection. A series of cell lines and primary cells were identified that require Axl for optimal ZEBOV entry. Using one of these cell lines, we identified ZEBOV entry events that are Axl-dependent. Interactions between ZEBOV-GP and the Axl ectodomain were not detected in immunoprecipitations and reduction of surface-expressed Axl by RNAi did not alter ZEBOV-GP binding, providing evidence that Axl does not serve as a receptor for the virus. However, RNAi knock down of Axl reduced ZEBOV pseudovirion internalization and α-Axl antisera inhibited pseudovirion fusion with cellular membranes. Consistent with the importance of Axl for ZEBOV transduction, Axl transiently co-localized on the surface of cells with ZEBOV virus particles and was internalized during virion transduction. In total, these findings indicate that endosomal uptake of filoviruses is facilitated by Axl.

© 2011 Elsevier Inc. All rights reserved.

Introduction

The filoviruses *Ebolavirus* and *Marburgvirus* have caused a number of devastating hemorrhagic fever outbreaks in Africa over the past 30 years. These enveloped, non-segmented, negative-stranded RNA viruses are listed as Category A biodefense agents due to the significant mortality associated with infection. No vaccines or antiviral therapies are currently available against these viruses. A better understanding of the cellular proteins that are required for filovirus entry into cells may lead to strategies to combat these pathogens.

The *Zaire ebolavirus* (ZEBOV) and *Lake Victoria marburgvirus* (MARV) glycoproteins (GP) facilitate pseudovirus entry into a broad range of cell types from many mammalian species (Wool-Lewis and Bates, 1998). This wide tropism has complicated the identification of cellular proteins required for filovirus entry. Nonetheless, several different plasma membrane-associated proteins have been identified to enhance filovirus infection/transduction. The C-type lectins have been shown to increase entry into some cells (Alvarez et al., 2002;

Baribaud et al., 2002; Geijtenbeek and van Kooyk, 2003; Lasala et al., 2003; Lin et al., 2003; Marzi et al., 2004; Simmons et al., 2003a; Takada et al., 2004), but many highly permissive cells do not contain C type lectins leading investigators to conclude that this group of plasma membrane-associated proteins serve as adherence factors rather than receptors that mediate virus entry. Folate receptor-α was identified to enhance ZEBOV-GP pseudovirion entry when the protein was ectopically expressed in Jurkat cells (Chan et al., 2001); however, this protein was subsequently shown to be unnecessary in a number of permissive cells (Simmons et al., 2003b; Sinn et al., 2003). Most recently, the tyrosine kinase receptor Axl was identified to facilitate ZEBOV and MARV transduction of some but not all permissive cell lines (Shimojima et al., 2007; Shimojima et al., 2006).

Axl is one of three members of the TAM (Tyro3, Axl, Mer) protein family (Linger et al., 2008). These proteins are single pass, type 1 plasma membrane-associated proteins. The ectodomain consists of two immunoglobulin-like domains as well as and two fibronectin-like domains (Linger et al., 2008). The two immunoglobulin-like domains are responsible for TAM family interactions with three known ligands or groups of ligands, the Tubby family of proteins, Gas6 and Protein S (Caberoy et al., 2010; Heiring et al., 2004; Sasaki et al., 2006; Stitt et al., 1995; Varnum et al., 1995). These ligand/Axl interactions lead to receptor homo- and heterodimerization of Axl, Mer and Tyro3 and subsequent tyrosine-dependent signaling. Specifically, Gas6/Axl ligation results in a variety of cell type-dependent effects including cell

* Corresponding author at: 3-750 Bowen Science Building, Department of Microbiology, University of Iowa, Iowa City, IA 52242, USA. Fax: +1 319 335 9006.

E-mail address: wendy.maury@uiowa.edu (W. Maury).

¹ Current address: Department of Pediatrics, Emory University School of Medicine and Children's Healthcare of Atlanta, Atlanta, GA 303221, USA.

² Authors contributed equally to this work.

migration/chemotaxis (Fridell et al., 1998; Zhang et al., 2008), adhesion (McCloskey et al., 1997), cell survival (Zheng et al., 2009) and division (Lee et al., 1999).

While no direct interactions between ZEBOV-GP pseudovirions and Axl have been demonstrated, site-directed mutagenesis of Axl identified residues in both the ectodomain and the cytoplasmic tail that are required for enhanced ZEBOV-GP pseudovirion transduction (Shimojima et al., 2007). The requirement of Axl cytoplasmic tail residues suggests Axl signaling may be involved in Axl-dependent ZEBOV-GP transduction. We recently demonstrated that Axl enhances bulk fluid phase uptake or macropinocytosis of cargo as diverse as 70 kDa dextran, ZEBOV-GP pseudovirions, ZEBOV virus-like particles (VLPs) and infectious ZEBOV. Axl-dependent macropinocytosis required actin polymerization and was profoundly inhibited by the amiloride analog EIPA (Hunt et al., 2011).

In a large screen of human tumor cell lines that correlated cellular gene expression with ZEBOV-GP pseudovirion transduction, we found that Axl expression positively correlated with ZEBOV-GP-dependent transduction, but not vesicular stomatitis virus (VSV)-G-dependent. To better understand the role of Axl in filovirus entry, we identified steps involved with ZEBOV-GP-dependent transduction that require Axl expression. Our findings indicate that Axl does not directly interact with ZEBOV-GP but instead facilitates filovirus internalization and membrane fusion, consistent with a newly appreciated role of Axl in macropinocytosis.

Results

AXL mRNA expression correlates with ZEBOV-GP-mediated transduction of the NCI-60 panel of human tumor cells

To identify proteins important for ZEBOV-GP-mediated entry, we performed Gene Correlation Analyses (CGA) using the NCI-60 panel of human tumor cells. CGA screens have previously identified cellular receptors for adeno associated virus 5 and 6 and implicated the GTPase RhoC with enhancing both ZEBOV and VSV transduction (Di Pasquale et al., 2003; Quinn et al., 2009; Weller et al., 2010). This bioinformatics-based approach correlated virus transduction with gene expression in the NCI-60 cell panel. VSV/EGFP virions pseudotyped with either mucin domain deleted ZEBOV glycoprotein (ZEBOV-GP ΔO VSV) or VSV-G (VSV-G VSV) were transduced into 52 of the NCI-60 cell lines. ZEBOV-GP ΔO that has the mucin domain of the glycoprotein deleted was used in this screen and most of the other experiments in this study because it contains the intact viral glycoprotein receptor binding domain, confers entry in a manner similar to the full-length glycoprotein but produces titers that are consistently higher (Jeffers et al., 2002).

The relative mean transduction values of three independent experiments were used as a seed file and compared with gene array data from the NCI-60 panel that is publically available at <http://www.dtp.nci.nih.gov/compare/>. Using a Pearson correlation analysis, a list of cellular genes that strongly and positively correlated with ZEBOV-GP-dependent transduction was generated. Those cellular genes whose expression were associated with ZEBOV-GP ΔO VSV transduction with a highly positive Pearson correlation coefficient (PCC) were further delimited using EnTuned software to identify function, subcellular location, and pathway associations since we were interested in genes that expressed plasma membrane-associated proteins (http://www.macresearch.org/entuned_pl). Additionally, genes that highly correlated with transduction of both ZEBOV-GP and VSV-G pseudovirions were discarded under the assumption that these genes encoded proteins involved in VSV uncoating and/or expression and were not genes directly pertinent to ZEBOV-GP-dependent entry.

A number of genes were identified that encoded plasma membrane-associated proteins that correlated with ZEBOV-GP pseudovirion transduction but did not correlate with VSV-G pseudovirion transduction. Expression of one gene that correlated strongly was the Tyro3/Axl/

Mer (TAM) family member *AXL* (Fig. 1A). ZEBOV-GP-dependent transduction of the cell panel, but not VSV-G-dependent transduction demonstrated a similar trend to that observed with *AXL* mRNA expression (Fig. 1B and C). *AXL* mRNA expression in the NCI-60 panel correlated with ZEBOV-GP-mediated transduction with a PCC of 0.517 that was found to be highly statistically significant ($p < 0.001$). Axl had been previously identified to facilitate filovirus entry in a cDNA screen performed by Shimojima et al. (2006). While Shimojima et al. demonstrated that the other two TAM family members Dtk (also called Tyro3) and Mer can also enhance ZEBOV-GP-dependent transduction into poorly permissive cells (Shimojima et al., 2006), neither Tyro3 nor Mer positively correlated with ZEBOV-GP-dependent transduction in our screen. Interestingly, folate receptor- α that is implicated in filovirus entry did not correlate with ZEBOV-GP-dependent transduction in this screen.

To validate the NCI-60 microarray correlation findings, we initially evaluated cell surface expression of Axl on two of the cell lines identified by the gene array to have high *AXL* mRNA expression and two lines with low *AXL* mRNA expression. Axl protein expression levels as assessed by binding of polyclonal antisera directed against the Axl ectodomain to live cells in a flow cytometric assay were consistent with the microarray data. M14 and UACC-257 (#3 and #7 melanoma lines in Fig. 1, respectively) that had little or no *AXL* mRNA expression did not have detectable Axl on their surface (Fig. 2A). In contrast, SNB-19 and SN12C (#4 CNS line and #6 renal line in Fig. 1) that had abundant *AXL* mRNA expression in the gene array expressed large quantities of cell surface Axl (Fig. 2B). Evaluation of Axl surface expression on other NCI-60 lines was also consistent with the gene array results (data not shown). To further appraise Axl expression on primary cell populations, human foreskin fibroblasts (Hff) and human umbilical vein endothelial cells (HuVEC) were examined and found to express readily detectable levels of cell surface Axl (Fig. 2C). These same six cell populations were also assessed for both Tyro3 and Mer expression and none of them was found to express the other two TAM family members (data not shown).

Axl enhancement of ZEBOV-GP-mediated infection is cell type-specific

To examine the requirement for Axl in ZEBOV-GP-mediated entry, we utilized polyclonal antisera directed against the Axl ectodomain that has been shown to inhibit ZEBOV-GP-dependent transduction in some cells (Shimojima et al., 2006). VSV-G pseudovirions served as controls in these studies since Axl expression did not positively correlate with VSV-G-dependent transduction in our CGA. We used Vero and 293T cells that do not require Axl expression for optimal ZEBOV pseudovirion transduction as negative controls in this study (Shimojima et al., 2006). As previously demonstrated (Shimojima et al., 2006), we found that 293T cells do not express Axl, whereas Vero cells express significant levels of surface Axl, but Axl expression has no effect on ZEBOV transduction (data not shown). In addition to transducing these cells, we extended our studies to include two Axl-expressing lines from the NCI-60 panel as well as our Axl-expressing primary cells (Hffs and HuVECs). Cells were incubated with Axl antisera or normal goat sera (GS) and transduced with equivalent amounts of ZEBOV-GP ΔO or VSV-G VSV pseudovirions. Axl antisera significantly reduced ZEBOV-GP-dependent transduction of SNB-19, Hff, and HuVECs, but did not decrease transduction of 293T, Vero or SN12C cells (Fig. 3A). Thus, ZEBOV transduction was enhanced by surface availability of Axl in three of the Axl-expressing cell populations. Additionally, our findings with Vero and SN12C cells are consistent with the previous report that surface Axl expression does not predict that Axl will facilitate ZEBOV-GP-dependent uptake (Shimojima et al., 2006). Similar findings using Axl antisera incubated with these different cell populations were also observed with FIV pseudovirions bearing ZEBOV-GP (data not shown). This highlights the fact that the effect of Axl on ZEBOV transduction was

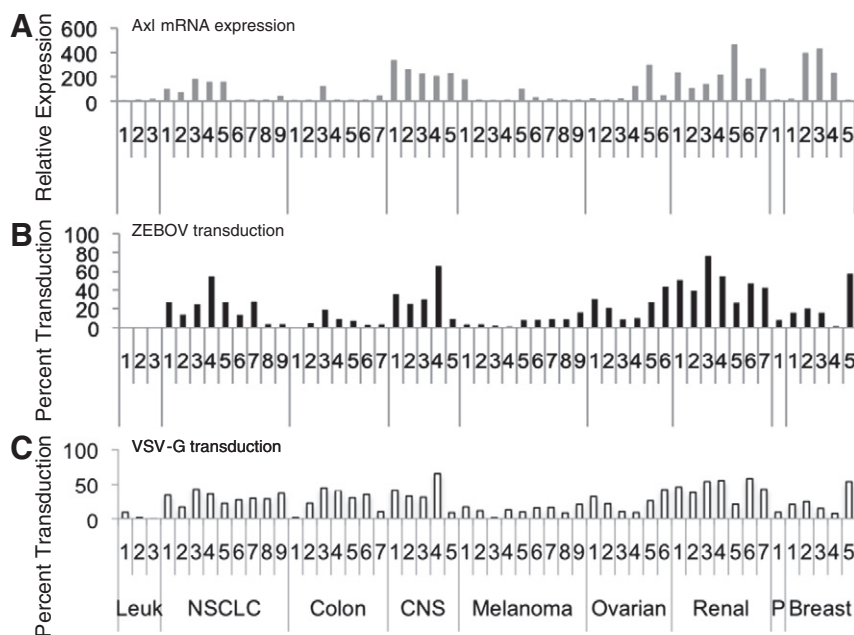


Fig. 1. Correlation of ZEBOV-GP pseudotyped VSV transduction with *AXL* expression in the NCI-60 panel of human tumor cells. (A) Relative expression of *AXL* mRNA expression in the 52 cell lines analyzed in the screen. (B) ZEBOV-GP Δ O VSV transduction of the 52 lines. (C) VSV-G VSV transduction of the same lines. *AXL* expression and ZEBOV-GP Δ O-dependent transduction, but not VSV-G-dependent transduction were positively correlated in our transduction screen with a Pearson correlation coefficient (PCC) of 0.517 ($p < 0.0001$). Data shown are the mean of three independent sets of transductions. Gene array data from the individual arrays are available at <http://www.dtp.nci.nih.gov/mtargets/download.html>. The data set compared in this study was GC11900. Leuk = leukemia lines; NSCLC = non-small cell lung carcinoma; CNS = central nervous system; P = prostate.

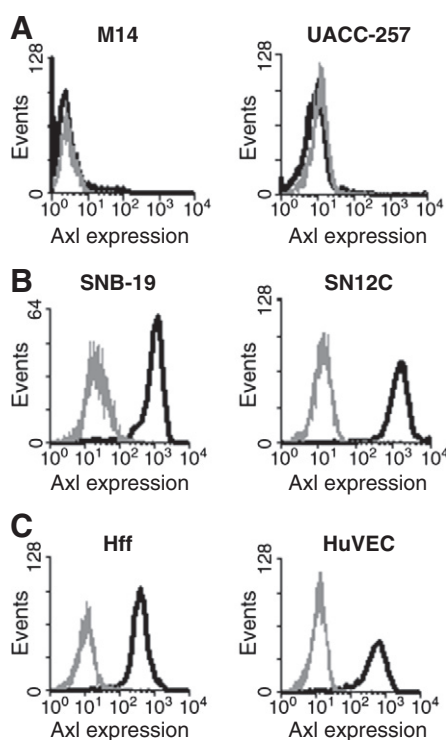


Fig. 2. Cell surface Axl expression. (A) Axl surface expression on two NCI-60 cell lines that were poorly transduced with ZEBOV-GP Δ O VSV and displayed low levels of *AXL* expression in NCI-60 gene array studies. (B) Axl surface expression on two NCI-60 cell lines that were highly transduced with ZEBOV-GP Δ O VSV and displayed robust levels of *AXL* mRNA expression on the gene arrays. (C) Axl expression on the surface of two primary human cell populations, human foreskin fibroblasts (Hff) and umbilical cord endothelial cells (HuVEC). Cells stained with normal goat sera are shown in gray histograms, whereas cells stained with goat anti-human Axl antisera are shown in black histograms.

independent of the viral core particle used. As a result of this consistent finding, we used both VSV and FIV pseudovirions in this study.

Surprisingly, we found that VSV-G transduction into SN12C, Hffs and HuVECS was decreased by Axl antibodies. SNB-19 cells that had reduced ZEBOV-GP-dependent entry in the presence of Axl antisera did not have reduced VSV-G transduction in the presence of the antisera. This finding is consistent with our previously published studies using RNAi knock down of Axl (Hunt et al., 2011). Interestingly, both ZEBOV-GP- and VSV-G-dependent entry were inhibited by anti-Axl antibodies in the primary cell populations.

Enhancement of ZEBOV transduction by surface expression of Axl

We recently showed that RNAi knock down of endogenous *AXL* expression reduced replication of infectious ZEBOV by 80% during a 20 h virus infection, directly demonstrating the importance of Axl for optimal ZEBOV entry into some cells (Hunt et al., 2011). As these initial studies only evaluated ZEBOV infection during a single round of infection, we sought to determine if Axl antisera effectively decreased ZEBOV infection over a longer term infection. In these studies, a recombinant, infectious VSV was generated that has the G gene replaced with ZEBOV-GP Δ O and EGFP (ZEBOV-GP-VSV/EGFP) that allowed us to assess virus replication under BSL2 conditions. These studies were performed in SNB-19 cells that are part of the NCI-60 panel (CNS cell line #4, Fig. 1) and served as a model cell type that requires Axl for optimal ZEBOV-GP transduction, but not VSV-G transduction. These cells express large quantities of Axl and can be readily transfected, providing an excellent cell line for understanding the role of Axl in ZEBOV infection. Axl antisera or GS was added 15 min prior to the addition of infectious ZEBOV-GP-VSV/EGFP (MOI = 0.1). EGFP positive cells in the cultures were assessed by flow cytometry at days 1–4 of infection. Axl antisera decreased the number of VSV infected cells at days 2 and 3, indicating reduced levels of initial infection and delayed spread of the virus (Fig. 3B). Thus, consistent with our earlier study (Hunt et al., 2011), loss of Axl availability on the surface of SNB-19 cells using Axl antisera also inhibits ZEBOV-GP-dependent infection.

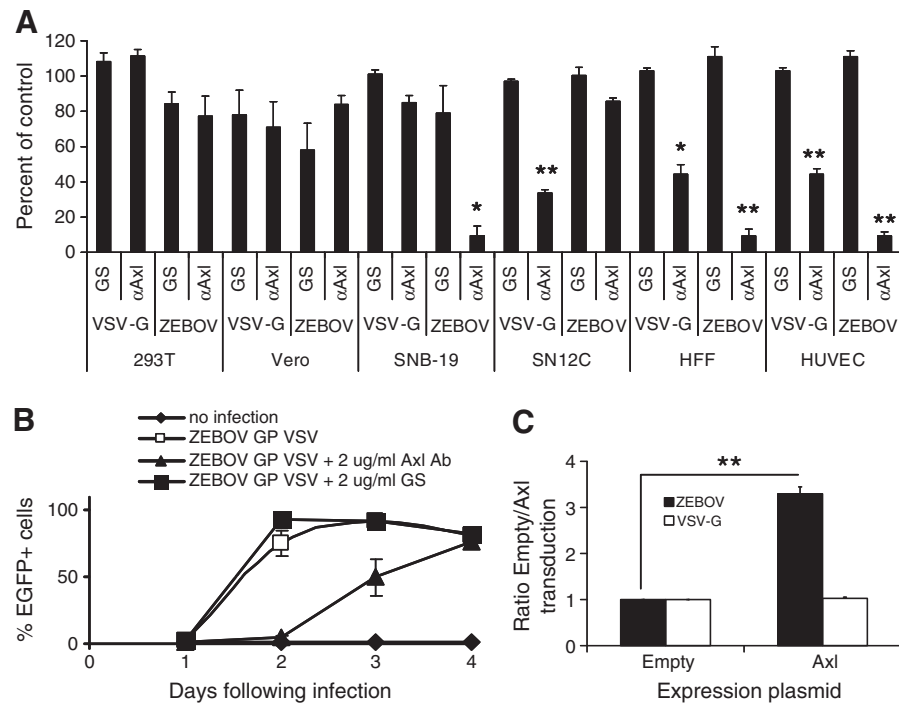


Fig. 3. The impact of Axl on ZEBOV transduction is cell dependent. (A) Ability of Axl antisera to block ZEBOV-GP- and VSV-G-dependent transduction. Cells were incubated with 8 µg/ml of goat anti-Axl sera or normal goat serum (GS) at 4 °C for 30 min. VSV-G or ZEBOV-GP ΔO pseudotyped VSV (MOI = 0.5) was added to cells and shifted to 37 °C. Twenty hours following transduction, the cells were analyzed for EGFP expression using flow cytometry. Relative transduction values in the presence of antisera are shown as the percent of transduction in the absence of antisera (control values) for each cell population. Shown are the mean and standard error of the mean of three independent experiments. * $p < 0.05$, ** $p < 0.001$. (B) Ability of Axl antisera to reduce infection of recombinant ZEBOV-GP ΔO VSV. SNB-19 cells were pre-incubated with either 2 µg/ml of anti-Axl antisera or normal goat sera (GS) for 15 min prior to addition of virus (MOI = 0.1). Cells were assessed for EGFP expression on days noted. Shown are the mean and standard error of the mean of one experiment that is representative of three independent studies that were performed. (C) Ability of Axl expression to increase ZEBOV-GP ΔO pseudotyped VSV entry in the poorly permissive NCI-H522 cell line. NCI-H522 cells were transfected with empty plasmid or plasmid expressing Axl and transduced with VSV pseudotypes (MOI 0.005) 48 h following transfection. Cells were analyzed for EGFP expression 24 h following transduction by flow cytometry. A ratio of transduction in the presence of Axl expression plasmid relative to transduction in the presence of empty plasmid is shown. Shown are the mean and standard error of the mean of three independent experiments. ** $p < 0.001$.

Previously, it has been shown that expression of Axl and other TAM family members enhanced the entry of ZEBOV into cells that were normally not permissive to ZEBOV (Shimojima et al., 2006). We thus sought to determine if expression of Axl could enhance ZEBOV-GP-mediated entry into additional cell populations identified in our current CGA screen as low AXL mRNA expressers and poorly permissive for ZEBOV transduction. We transfected two NCI-60 NSCLC populations, NCI-H460 and NCI-H522 (NSCLC cell lines #8 and 9, respectively, Fig. 1), with an empty expression vector or with an expression vector bearing Axl (Fig. 3C). Flow cytometric analysis of the transfected cells demonstrated cell surface expression of Axl in the Axl plasmid transfected populations (data not shown). Cells were transduced with ZEBOV-GP ΔO or VSV-G VSV (MOI = 0.005) at 48 h following transfection. The ratio of transduction in the presence of empty plasmid versus the Axl-expressing vector was then calculated after live cell assessment for EGFP by flow cytometry. A 3.5 fold increase in ZEBOV-GP-mediated transduction was observed in the NCI-H522 cells (Fig. 3C) whereas a more modest 1.7 fold increase was observed in NCI-H460 cells (data not shown). Transduction ratios of VSV-G VSV remained unchanged in both cell populations, indicating that transient expression of Axl in cells that do not normally express abundant levels of Axl allows for a specific enhancement of ZEBOV-GP-mediated entry.

Transduction of proteolytically processed ZEBOV pseudovirion requires Axl

Proteolytic processing of ZEBOV-GP1 is required for virion fusion to occur (Chandran et al., 2005; Schornberg et al., 2006). We inquired if

the requirement for Axl for optimal ZEBOV transduction into SNB-19 cells was affected by proteolytic processing of ZEBOV-GP pseudovirions. We transfected SNB-19 cells with either AXL RNAi or an irrelevant RNAi and transduced either full-length or thermolysin-treated full-length ZEBOV-GP VSV into the transfected cells. The ZEBOV-GP on virions mock or thermolysin-treated was immunoblotted to verify protease cleavage of the viral GP (Supplemental Fig. 1). AXL RNAi decreased the total amount of Axl protein present in SNB-19 cell lysates and reduced Axl on the surface of cells (Fig. 4A and B). As previously observed by others (Schornberg et al., 2006), thermolysin-treated virions had about 4-fold higher transduction than virions pseudotyped with untreated, full-length ZEBOV-GP. However, transduction into AXL RNAi-treated cells of either untreated or thermolysin-treated virions was reduced by approximately 55% indicating that the thermolysin-treated virions still required Axl for optimal transduction into SNB-19 cells (Fig. 4C).

ZEBOV-GP does not interact with the Axl ectodomain

Evidence demonstrated a requirement for Axl in some cells for optimal filovirus transduction, but direct interaction of ZEBOV-GP and Axl has not been shown. Co-immunoprecipitations (co-IPs) between Axl and ZEBOV-GP were performed to determine if we could detect direct interactions between the two proteins. The chimeric protein Axl-Fc was bound to Protein A beads and incubated with ZEBOV-GP ΔO pseudotyped FIV, baculovirus GP64 pseudotyped FIV or the endogenous Axl ligand Gas6. Neither of the two viral glycoproteins interacted with Axl-Fc (Fig. 5A); however, Gas6 bound to Axl-Fc indicating the immunoprecipitation conditions were appropriate for detection of ligand–receptor interactions.

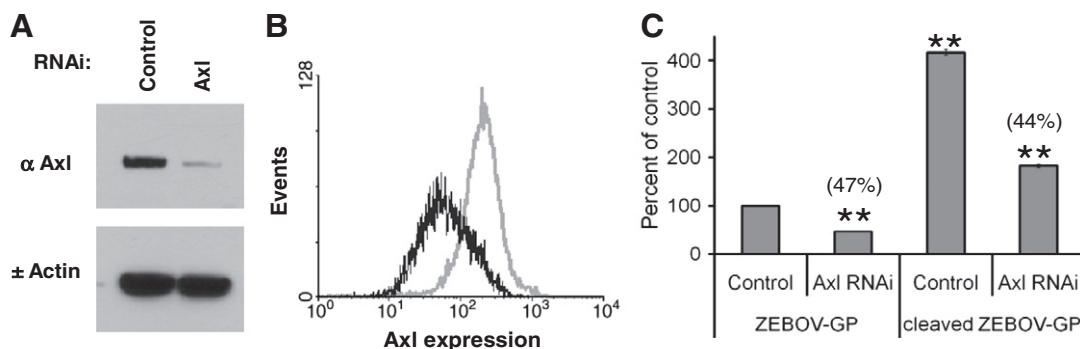


Fig. 4. Thermolysin-treated ZEBOV-GP pseudovirions remain sensitive to AXL RNAi treatment. (A and B) Knockdown of Axl expression in SNB-19 cells by validated AXL siRNA (Invitrogen) at 48 h following transfection as assessed by immunoblotting of cell lysates for Axl (A) or cell-surface expression of Axl (B). Shown in the black histogram are cells treated with AXL RNAi; the gray histogram represents cells treated with an irrelevant RNAi. (C) Thermolysin-treated full-length ZEBOV-GP FIV pseudovirions remain sensitive to AXL RNAi treatment. Virions were treated with thermolysin or mock-treated and added to SNB-19 cells that were treated with either AXL RNAi or an irrelevant RNAi. Cells were evaluated at 48 h following transduction for β -gal expression. The findings are shown as the number of transduced cells found in each treatment divided by the number of cells transduced by the untreated full-length ZEBOV-GP control. The numbers in parenthesis represent the effect of AXL RNAi treatment on transduction relative to the respective control. ** p <0.001.

To further explore possible interactions between ZEBOV-GP and Axl, co-IPs were repeated to determine if ZEBOV-GP pseudotyped virus could pull-down Axl from SNB-19 cell lysates. ZEBOV-GP Δ O pseudotyped FIV particles were bound to beads using anti-GP1 antibodies. SNB-19 cell lysates were incubated with the beads and bound proteins were identified by immunoblotting. Again, ZEBOV-GP failed to pull-down Axl from the cell lysates (Fig. 5B). As a cellular receptor for ZEBOV has yet to be identified, we were unable to provide a positive control for ZEBOV-GP co-immunoprecipitations in this study.

We also evaluated possible interactions of thermolysin-cleaved ZEBOV-GP with Axl. We verified that thermolysin treatment of virions produced the 19 kDa GP1 product (Supplemental Fig. 1) and evaluated viral particles for their ability to interact with Axl-Fc during a co-IP (Fig. 5C). Pre-cleaved virions also failed to interact with Axl. These studies provide a number of lines of evidence that ZEBOV-GP and Axl do not interact under the conditions tested.

Loss of Axl does not affect ZEBOV pseudovirion binding to SNB-19 cells, but decreases ZEBOV-GP pseudovirion internalization and fusion

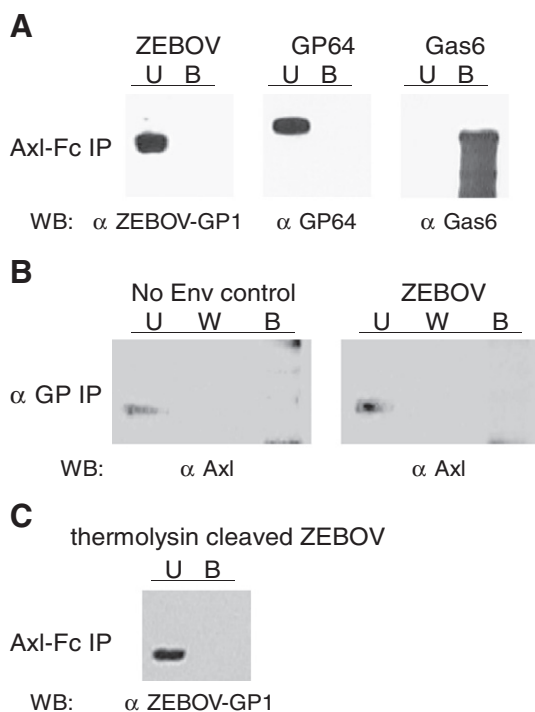


Fig. 5. Direct interactions between ZEBOV-GP and Axl cannot be detected. (A) Axl-Fc (0.5 μ g) was bound to Protein A sepharose beads and incubated with ZEBOV-GP Δ O or baculovirus GP64 pseudotyped FIV particles. Pull-down of Gas6 (0.5 μ g) served as a positive control in this study. U, unbound; B, Axl-Fc bound. (B) ZEBOV pseudotyped particles were bound to protein G beads with anti-ZEBOV-GP1 antisera. SNB-19 cell lysates were passed over the beads and the unbound (U), wash (W), and bound (B) fractions were examined for Axl by immunoblot. (C) Axl-Fc does not interact with thermolysin-cleaved ZEBOV FIV particles.

We could not detect direct interactions between Axl and ZEBOV-GP in pull downs; however, we also assessed Axl/ZEBOV-GP interactions by evaluating if loss of cell surface availability of Axl impacted ZEBOV-GP pseudovirion binding to SNB-19 cells. We first tested whether pre-incubation of commercially available, purified Axl-Fc (R&D Systems) with SNB-19 or 293T cells reduced ZEBOV transduction and found that this had no effect on transduction of either ZEBOV-GP Δ O or VSV-G VSV pseudovirion transduction into either cell type (Fig. 6A). In these studies, we used 293T cells as a negative control since Axl is not expressed in these cells. AXL RNAi knock down of Axl expression also had no effect on ZEBOV-GP Δ O FIV pseudovirion binding to SNB-19 cells (Fig. 6B). Finally, pre-treatment of SNB-19 cells with polyclonal Axl antisera did not reduce ZEBOV-GP Δ O pseudovirion binding to cells (data not shown). In total, our data provide no evidence that Axl directly interacts with ZEBOV-GP. Thus, it is unlikely that Axl serves as a cellular receptor for this virus.

We also determined if RNAi knock down of AXL inhibited ZEBOV-GP pseudovirion internalization. We treated cells with AXL RNAi or an irrelevant RNAi (Block-It, Invitrogen) and, 48 h later, ZEBOV-GP Δ O or VSV-G FIV pseudovirions were bound to SNB-19 cells for 1 h at 4 °C. The cells were washed to remove unbound virus. Under these conditions where no virions are internalized into cells, detection of cell-bound virions was completely abrogated by trypsin treatment (data not shown). Following a 2-h incubation of these virus-bound cells at 37 °C, cells were treated with trypsin to remove any virions that were not internalized, washed with PBS with 5% FCS and lysed. Lysates were immunoblotted for FIV capsid and cellular actin and the amount of each protein was quantified by ECL photon emission on the immunoblot. Amount of internalized virus was normalized to cell numbers using cellular actin signals. The data are shown as the amount of internalized virions in the presence of AXL RNAi divided the amount of internalized virions in cells treated with Block-It (Fig. 6C). We found that ZEBOV-GP Δ O pseudovirion internalization was reduced approximately 40% by AXL RNAi treatment. This provided

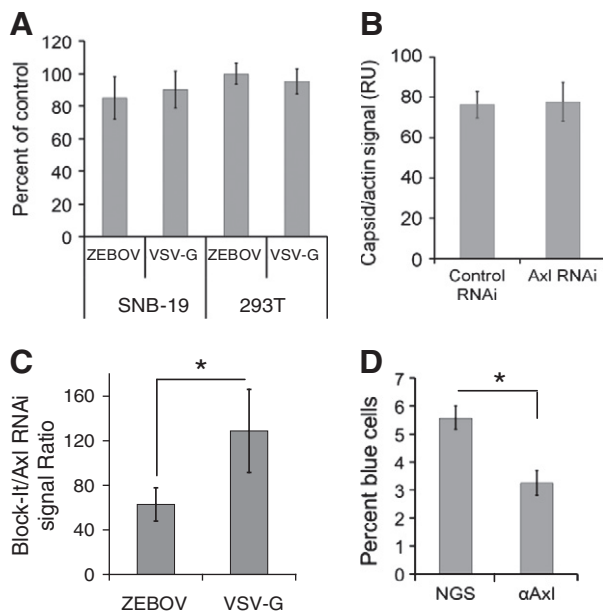


Fig. 6. Axl is required for post-binding events. (A) Soluble Axl-Fc does not interfere with ZEBOV-GP ΔO pseudotyped VSV transduction. ZEBOV and VSV-G virions were pre-incubated with Axl-Fc (50 μg/ml) and transduced on to Axl-dependent SNB-19 cells or the Axl-independent 293T cells. Transduction was evaluated by EGFP expression in the transduced populations at 24 h. Results are shown as the number of cells transduced in the presence of Axl-Fc divided by the number of transduced cells in the absence of treatment. (B) RNAi knock down of Axl had no effect on ZEBOV-GP ΔO pseudovirion binding. Forty-eight hours following transfection of *AXL* RNAi or an irrelevant RNAi into SNB-19 cells, equivalent quantities of ZEBOV-GP ΔO FIV were incubated with cells for 1 h at 4 °C. Unbound virus was removed and cells were lysed. Lysates were immunoblotted for FIV capsid and quantitated as described in Materials and methods. Shown are average pixel values of FIV capsid on the immunoblot divided by the average pixel values for cellular β-actin from 10 independent experiments. (C) ZEBOV-GP ΔO FIV internalization, but not VSV-G FIV is decreased in *AXL* siRNA-treated cells. SNB-19 cells were transfected with *AXL* siRNA or an irrelevant control siRNA. At 48 h, ZEBOV-GP ΔO FIV pseudovirions were bound to the cells for 1 h at 4 °C. Unbound virus was removed and cells were shifted to 37 °C for 2 h. Cells were lysed and immunoblotted for FIV capsid and cellular actin. The capsid signal was normalized for actin levels and data are reported as the ratio of the FIV signal in the Axl knock down cells divided by the FIV signal in the cells transfected with an irrelevant RNA. (D) Ability of Axl antisera to block ZEBOV VLP fusion events. ZEBOV-GP ΔO VLPs containing Src-β-lactamase were transduced into SNB-19 cells in the presence or absence of 1:20 dilution of polyclonal antisera against the ectodomain of Axl or normal goat sera (NGS). Entry of β-lactamase into the cytoplasm of cells was evaluated by flow cytometry following incubation of the cells with the fluorescent β-lactamase substrate CCF2/AM for 2 h. *p<0.05.

our first evidence that post-binding entry steps of ZEBOV are affected by Axl. Similar studies with VSV-G pseudovirions demonstrated that Axl knock down had no effect on internalization of these virions.

To further explore the effect(s) of Axl on ZEBOV-GP-mediated post-binding events, we assessed virion/endosomal membrane fusion using ZEBOV-GP ΔO bearing virus-like particles (ZEBOV ΔO VLPs). As virion fusion events are downstream from virion internalization events, we predicted that Axl antisera would also reduce fusion. ZEBOV ΔO VLPs were generated containing recombinant Src/β-lactamase protein as previously described (Quinn et al., 2009) and were used in these studies to complement our internalization findings using FIV cores rather than ZEBOV cores. In this assay, β-lactamase activity was detected by pre-loading the fluorescent β-lactam substrate CCF2/AM into the cytoplasm of SNB-19 cells. ZEBOV ΔO VLP fusion with endosomal membranes was measured by a change in fluorescence due to cleavage of the β-lactam ring (Cavrois et al., 2002; Cavrois et al., 2004). In a manner consistent with our FIV-based internalization assays, the addition of anti-Axl antisera decreased ZEBOV ΔO VLP fusion by about 40% compared to the normal GS (Fig. 6D). Thus, both virus internalization and fusion were reduced by

the loss of available surface-expressed Axl, indicating that Axl is involved in ZEBOV-GP-mediated entry at a post-binding step.

Axl internalizes as ZEBOV pseudovirions enter SNB-19 cells

To determine the localization of Axl during ZEBOV-GP ΔO pseudovirion entry, both pseudovirions and Axl were tracked in SNB-19 cells over a 45-min time course of ZEBOV-GP ΔO FIV transduction using confocal microscopy. Axl was found to be present primarily on the surface of naive SNB-19 cells (data not shown). A similar distribution of Axl was observed in cells that were cooled to 4 °C and incubated for 60 min with either ZEBOV-GP ΔO FIV (MOI = 250) (Figs. 7A and 8A) or FIV-VSV-G FIV (MOI = 250) (Supplemental Fig. 2). A high MOI was used in these studies to allow good confocal detection of virions using an anti-FIV capsid antibody. Cell surface co-localization of ZEBOV pseudovirions and Axl was evident during the initial 4 °C binding step in both permeabilized and non-permeabilized cells (Figs. 7A and 8A). Following this 1 h binding step, unbound virus was removed and cells were shifted to 37 °C for various times (Figs. 7B–D and 8B–D). At 15 min following the temperature shift, both Axl and ZEBOV-GP ΔO FIV pseudovirions remained almost exclusively on the cell surface and frequent co-localization was still observed. By 30 min, both virions and Axl appeared to be internalized since decreased FIV capsid and Axl signals were consistently observed in non-permeabilized cells (Fig. 8C) and, in the permeabilized cells, expression of both antigens appeared distributed throughout the cell (Fig. 7C). At 30–45 min, little co-localization of the two signals occurred and, by 45 min, while much of the Axl remained intracellular, a portion of Axl appeared to be surface expressed again, suggesting the possibility that some was recycled to the surface of the cells (Figs. 7D and 8D). Combined, these studies provide evidence of internalization of both virions and Axl during virion infection, although co-localization of the two signals within cells did not occur.

Parallel confocal microscopy studies were performed with SNB-19 cells incubated with FIV virions pseudotyped with no viral glycoprotein and FIV virions pseudotyped with VSV-G. Axl and non-enveloped virions did not co-localize under these conditions at any time and, as expected, were unable to enter the cells at any point (data not shown). Surprisingly, we observed co-localization of VSV-G pseudovirions and Axl on the surface of cells at the zero time point. Much of this co-localization of the two signals was lost by 15 min at 37 °C (Supplementary Fig. 2). Unlike the ZEBOV-GP pseudovirion studies, as virions became intracellular over the 45 min, a parallel internalization of Axl was not observed. Instead, Axl remained primarily cell surface associated, suggesting that Axl was not internalized with the VSV-G pseudovirions.

Discussion

In a bioinformatics-based screen using a large panel of human tumor cells, Axl expression strongly correlated with ZEBOV-GP pseudovirion transduction. Axl was previously characterized to enhance filovirus entry into some cell populations (Shimojima et al., 2006) and, in a similar manner, we also observed that surface expression of Axl enhances ZEBOV pseudovirion entry into some cells. Using multiple approaches to inhibit Axl, we provided evidence that ZEBOV pseudovirion internalization and subsequent fusion are inhibited by loss of surface Axl expression. The impact on virus internalization did not appear to be due to direct Axl interaction with ZEBOV-GP pseudovirions or reduced ability of ZEBOV pseudovirions to interact with permissive cells, suggesting that Axl was stimulating ZEBOV-GP pseudovirion uptake through indirect mechanisms rather than serving as a receptor for ZEBOV. Consistent with a role for Axl in ZEBOV internalization, Axl and virions concomitantly internalized during pseudovirion entry.

Both ZEBOV pseudovirion internalization and membrane fusion were decreased by about 40% with the reduction of Axl on the surface of SNB-19 cells as assessed by *AXL* RNAi and Axl-specific antisera using

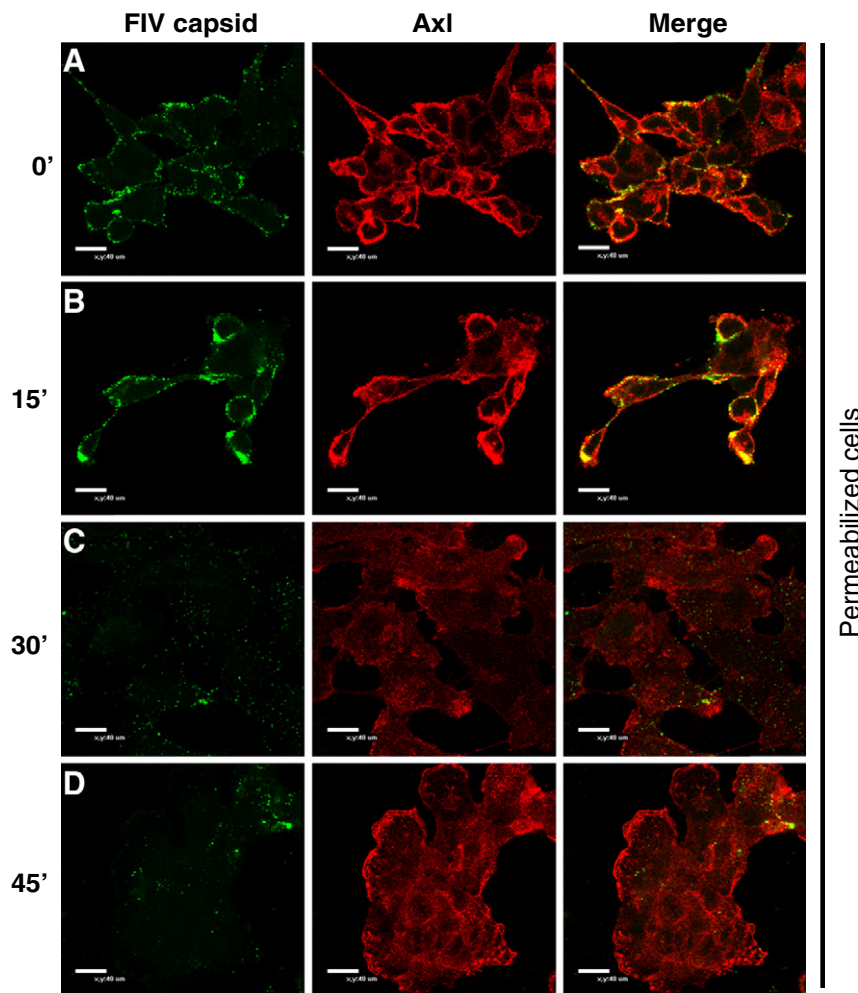


Fig. 7. Axl transiently associated with ZEBOV-GP Δ O pseudovirions on the cell surface and was internalized as virions entered cells. Confocal microscopy of Axl and FIV capsid during ZEBOV-GP Δ O FIV transduction. (A) Localization of Axl and FIV capsid expression in SNB-19 cells incubated with ZEBOV-GP Δ O FIV (MOI = 250) for 1 h at 4 °C. (B–D) Localization of Axl and FIV capsid in SNB-19 cells following incubation of ZEBOV-GP Δ O FIV (MOI = 250) for 1 h at 4 °C, removal of unbound virions and incubation of cells with pre-warmed media at 37 °C for 15 min (B), 30 min (C) or 45 min (D). All coverslips were fixed with 2% paraformaldehyde, permeabilized with 0.2% Triton X-100 and immunostained with goat anti-Axl and mouse anti-FIV capsid. Findings shown in panels are representative experiments performed three independent times.

two different virion model systems (Fig. 6C–D). As the effect on both of these steps results in a similar level of inhibition, it is likely that the effect occurs at the upstream event, internalization, and that fusion is affected as a result of reduced internalization. The modest impact on both of these entry events was associated with significantly decreased/delayed virus replication using a single administration of Axl antisera prior to initiation of infection (Fig. 3B). It is surprising that a 40% decrease in these entry events resulted in a complete loss of detectable infection at 2 days following infection. One possible explanation is that additional steps in virus replication that were not evaluated in these studies are inhibited by loss of cell surface Axl in addition to virus internalization.

We recently demonstrated that Axl stimulates bulk fluid phase uptake or macropinocytosis (Hunt et al., 2011). Loss of Axl-dependent macropinocytosis resulted in not only decreased uptake of ZEBOV pseudovirions, but other cargos such as large molecular weight dextran. Thus, we propose that greater numbers of ZEBOV particles bound to or in proximity with the surface of SNB-19 cells are internalized into endosomes due to Axl-dependent macropinocytosis, resulting in higher levels of virus infectivity. While our studies indicated that Axl-dependent macropinocytosis is important for enhanced ZEBOV entry (Hunt et al., 2011), the trigger(s) that stimulate macropinocytosis have yet to be identified.

Several lines of evidence suggest that cell signaling pathways are activated during Axl-dependent enhancement of ZEBOV-GP-mediated transduction. Shimojima et al. demonstrated that deletions in the cytoplasmic tail of Axl reduced Axl-mediated enhancement of ZEBOV-GP pseudovirion transduction, arguing that cell signaling is critical for Axl-enhanced ZEBOV infection (Shimojima et al., 2007). Our studies demonstrated that phospholipase C inhibitors specifically inhibited ZEBOV pseudovirion transduction in Axl-dependent cells, but not in cells where Axl does not enhance ZEBOV transduction (Hunt et al., 2011).

Signaling through Axl activation has been almost exclusively studied using the endogenous Axl ligand Gas6. Gas6 binding to Axl leads to a variety of cell-dependent biological outcomes including cytoskeleton rearrangements, cell migration, cell survival and division (Demarchi et al., 2001; Goruppi et al., 2001; Goruppi et al., 1997, 1999; Melaragno et al., 2004; Nielsen-Preiss et al., 2007; Zheng et al., 2009). Prior to our study (Hunt et al., 2011), a role for Axl in macropinocytosis had not been appreciated; however, TAM family member Mer is known to activate phagocytosis in macrophages (Scott et al., 2001; Shao et al., 2009). While co-IPs have demonstrated that the phosphorylated tyrosines in the cytoplasmic tail of TAM proteins interact with p85alpha and p85beta subunits of PI3K, PLC γ , RanBPM, Grb2 and Src (Braunger et al., 1997; Hafizi et al., 2005), Gas6/Axl interactions have

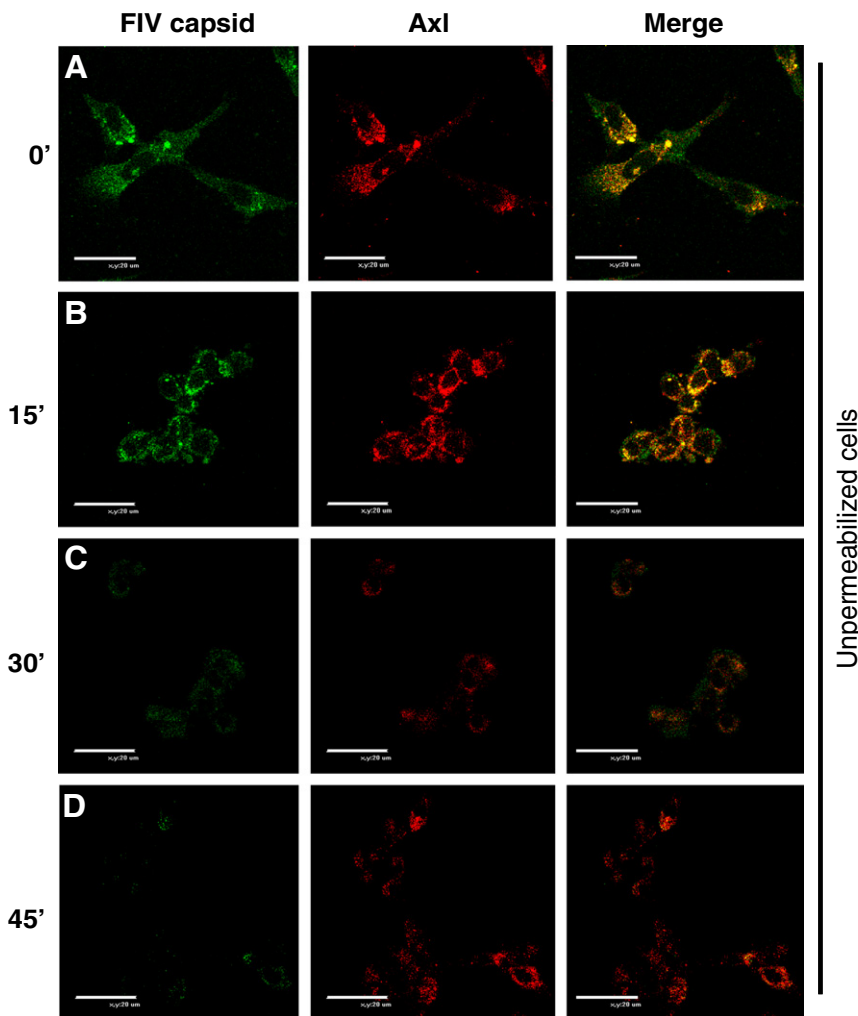


Fig. 8. Both Axl and ZEBOV-GP Δ O pseudovirions are internalized from the cell surface during infection. Confocal microscopy of Axl and FIV capsid during ZEBOV-GP Δ O FIV transduction in non-permeabilized cells. (A) Localization of Axl and FIV capsid expression in SNB-19 cells incubated with ZEBOV-GP Δ O FIV (MOI = 250) for 1 h at 4 °C. (B–D) Localization of Axl and FIV capsid in SNB-19 cells following incubation of ZEBOV-GP Δ O FIV (MOI = 250) for 1 h at 4 °C, removal of unbound virions and incubation of cells with pre-warmed media at 37 °C for 15 min (B), 30 min (C) or 45 min (D). All coverslips were fixed with 2% paraformaldehyde and immunostained with goat anti-Axl and mouse anti-FIV capsid. Findings shown in panels are representative experiments performed three independent times.

only been shown to result in signaling through PI3K, Src and Grb2 (Demarchi et al., 2001; Goruppi et al., 2001; Goruppi et al., 1997, 1999; Lee et al., 1999; Mellaragno et al., 2004; Son et al., 2007; Weinger et al., 2008; Wilhelm et al., 2008; Zheng et al., 2009). As stimulation of Axl-dependent macropinocytosis that enhanced ZEBOV infection did not require activation of the PI3K/Akt pathway, but phospholipase C-dependent pathways (Hunt et al., 2011), Axl signaling appears to occur through at least two different signaling pathways, leading to different physiological consequences. Recently, a new group of ligands for the TAM family kinases was identified (Cabroy et al., 2010). The Tubby protein interacts only with Mer, whereas tubby-like protein1 (Tulp1) interacts with all three TAM family members. Tubby contains elements that are essential for Mer binding, phosphorylation and phagocytosis activation. Tulp1 contains all of these functional elements as well, and is capable of binding to Axl in vitro. Additionally, activation of PLC γ and PLC β have been linked to Tubby protein activation (Carroll et al., 2004). However, it is not clear whether Tulp1 binding to Axl activates Axl signaling and is the ligand responsible for Axl-induced macropinocytosis. Further, it is not known if Tulp1/Axl interactions lead to PLC activation or whether other downstream signaling is activated by this interaction. While it is enticing to speculate that Tulp1 may be activating Axl and thereby stimulating macropinocytosis, this has yet to be directly demonstrated.

While recent studies suggest that a novel ligand may be responsible for activating Axl-dependent macropinocytosis leading to increased uptake of ZEBOV, an alternative Axl interaction may also stimulate ZEBOV entry. The Axl ectodomain is known to heterodimerize with IL-15-bound IL-15 receptor leading to active Axl signaling (Budagian et al., 2005). Thus, it is also possible that ZEBOV-GP may stimulate Axl signaling events as a result of binding to a currently unidentified receptor that in turn heterodimerizes with Axl. Such interactions may lead to activation of downstream signaling pathways. Such a model would also be consistent with a role for Axl in ZEBOV virion internalization.

As Shimojima et al. have shown (Shimojima et al., 2006), we observed that Axl enhances ZEBOV-GP-dependent transduction in some cells, but not others. While some cells such as 293T cells do not express Axl, other Axl-independent cells do express Axl, but expression of the protein does not enhance ZEBOV entry. Cell lines such as VeroE6 (Shimojima et al., 2006), Vero and SN12C express Axl on their plasma membrane, but Axl expression does not affect ZEBOV-GP-dependent transduction of these cells. It is possible that pathways connecting Axl to macropinocytosis may be disrupted in these transformed cell lines. In contrast, other Axl-expressing cells such as SNB-19 cells that have roughly equivalent levels of surface-expressed Axl as SN12C cells have a strong dependence upon Axl for optimal

ZEBOV-GP-mediated transduction. Thus, the transduction requirement for Axl in each permissive cell population needs to be empirically determined. We also demonstrated here that in two primary human cell populations (Hffs and HuVECs), optimal ZEBOV-GP-mediated transduction requires Axl. These initial studies with primary cell populations suggest the possibility that Axl may be important for *in vivo* filoviral infection and pathogenesis.

As proteolytic cleavage of ZEBOV-GP might abrogate the need for Axl, we investigated the effect of thermolysin cleavage of GP1 on the requirement of Axl (Fig. 4C). We found that while virions that were protease pre-treated had higher levels of transduction, entry of these particles was just as sensitive to the loss of Axl as particles containing full-length ZEBOV-GP. Thus, we concluded that the requirement for Axl is independent of requisite proteolytic pathways needed for productive ZEBOV transduction.

In our initial assessment of filovirus transduction of Axl-expressing cells, VSV-G pseudotyped virions were used as a negative control. Unexpectedly, VSV-G-dependent entry into some cells was reduced about two-fold by Axl antisera (Fig. 3A). This was a more modest impact than that observed for ZEBOV-GP transduction, but statistically significant. This finding provides additional evidence that the involvement of Axl in ZEBOV-GP-mediated entry is likely to due to indirect interactions with the virions rather than direct viral glycoprotein/receptor interactions. Even more surprising was our observation that some cells that required Axl for ZEBOV-GP-dependent entry did not require it for VSV-G-dependent entry and, conversely, other cell lines required Axl for VSV-G-dependent entry but not uptake mediated by ZEBOV-GP. One possible explanation for this finding is that uptake pathways utilized by these viruses may differ in these various cells. As we have demonstrated that Axl expression enhances macropinocytosis, but not other uptake pathways (Hunt, et al. 2011), we would propose that macropinocytosis also mediates VSV-G-dependent uptake into some cells. Consistent with the possibility, Bhattacharyya et al. demonstrated that VSV-G entry into some cells does not utilize clathrin coated pits, an entry pathway that has been well established for VSV-G entry into many cells (Bhattacharyya et al., 2010). Of note, entry of both pseudovirions into the primary cells, Hffs and HuVECs, was enhanced by Axl expression. Therefore, further exploration of uptake mechanisms of these viruses in other relevant primary cells such as macrophages and dendritic cells is warranted.

Material and methods

Cell lines

Cell lines from the NCI-60 panel (dtp.nci.nih.gov/docs/misc/common_files/cell_list.html) were examined for their ability to support mucin domain deleted ZEBOV-GP (ZEBOV-GP ΔO) pseudovirion transduction. All NCI-60 cells were maintained in RPMI with 5% FCS and pen/strep. Human umbilical vein endothelial (HuVEC) cells were isolated from a fresh umbilical cord and maintained in EBM media (Lonza/Cambrex) supplemented with the EBM bullet kit. Human foreskin fibroblasts (Hffs) (ATCC, CRL-1635) were grown in DMEM with 15% FCS and pen/strep.

Antibodies and Fc molecules

Antibodies were purchased commercially when possible. These included goat anti-Axl (#AF154, R&D Systems), mouse anti-FIV capsid monoclonal antibody (NIAID AIDS Research and Reference Reagent Program), feline anti-FIV polyclonal antibody (obtained locally from FIV seropositive cats), mouse anti-baculovirus gp64 monoclonal antibody (14-6995-81; eBioscience), mouse anti-human β-actin (ab49900-100; Abcam). Rabbit anti-ZEBOV-GP1 was kindly provided by A. Sanchez, CDC. Axl-human Fc (Axl amino acids 33–440 attached to human Fc) was purchased from R&D Systems (#154AL).

Pseudotyped particles

Pseudotyped VSV particles

Production of vesicular stomatitis virus (VSV) particles that were pseudotyped with either ZEBOV-GP ΔO or VSV-G was performed as previously described (Takada et al., 1997). Briefly, 293T cells were seeded into 15 cm dishes. The following day 75 μg of the glycoprotein expression plasmid were transfected into the cells using calcium phosphate transfection as previously described (Brindley et al., 2007). Twenty-four hours following transfection, the cells were washed twice in PBS and transfected 293Ts were transduced with pseudotyped VSV/EGFP/ΔG that expresses EGFP in place of the G glycoprotein at an MOI of 5. Six hours after transduction, the virus inoculum was removed and cells were again washed with PBS. Cell supernatants were collected at 24, 36, and 48 h following transduction. Stocks were filtered, aliquoted, and stored at –80 °C until use.

FIV pseudotyped particles

Pseudotyped FIV viral particles were produced as previously described (Brindley et al., 2007; Sinn et al., 2003). 293T cells were transfected with a total of 75 μg of DNA consisting of plasmids expressing one of three glycoproteins (full-length ZEBOV-GP, ZEBOV-GP ΔO or VSV-G), a FIV gag-pol expressing construct (pFIVΔΔ), and a packageable FIV genome that expressed β-galactosidase (pFIVψβgal) at a ratio of 1:2:3, respectively. The DNA was transfected into 15 cm dishes of 293T cells using calcium phosphate transfection. Supernatants were collected at 24, 36, 48, 60 and 72 h following transfection. The supernatants were filtered through a 0.45 μ filter and pelleted by an overnight centrifugation step (7000 rpm 4 °C in a Beckman JA-10 rotor). The viral pellet was resuspended in DMEM for an approximate 200 fold concentration. The virus was either used immediately for transduction or stored at –80 °C until use.

ZEBOV VLPs

Src-β-lactamase incorporated mucin domain deleted ZEBOV virus-like particles (ZEBOV ΔO-VLPs) were produced by transfecting 293T cells grown in 15 cm dishes with 75 μg of total DNA at a ratio of 1:2:3:3 for plasmids expressing ZEBOV-NP, ZEBOV-VP40, ZEBOV-GP ΔO and src-β-lactamase fusion protein (Quinn et al., 2009). pNP and pVP40 were kind gifts from Dr. Ronald Harty (University of Pennsylvania). Supernatants were collected at 24, 36, 48, 60 and 72 h following transfection. The supernatants were filtered through a 0.45 μ filter and pelleted by an overnight centrifugation step (7000 rpm 4 °C in a Beckman JA-10 rotor). The viral pellet was resuspended in DMEM for an approximate 200 fold concentration. The virus was stored at –80 °C until use.

NCI-60 screen

4×10^4 cells of 52 cell lines used from the NCI-60 panel (http://www.dtp.nci.nih.gov/docs/misc/common_files/cell_list.html) were plated in 48-well plates. Relative transduction efficiency was measured using VSV/EGFP/ΔG particles pseudotyped with either VSV-G or ZEBOV-GP ΔO. Twenty h following transduction the cells were evaluated for EGFP expression by flow cytometry to obtain the transduction efficiency for each cell line. The average of a total of six transduction trials was used as the seed file for COMPARE analysis against the GC235133 gene array data set that used the Affymetrix U133A chip (dtp.nci.nih.gov/docs/misc/common_files/cell_list.html).

Flow cytometry

EGFP expression

Twenty h following transduction, cells were lifted in 150 μl of Accumax (Fisher Scientific) and analyzed with a FACScan flow cytometer (Becton Dickinson) for FL-1 intensity.

Axl staining

Cells were lifted with PBS and 5 mM EDTA and washed 3 times in PBS/5% FCS. Cells were incubated with goat anti-Axl (4 µg/ml) or normal goat sera for 1 h on ice. Cells were washed and incubated with Cy5-conjugated donkey anti-goat (1:50) (Jackson Immunoresearch) for 30 min on ice. Cells were washed and analyzed with FACScan flow cytometer for FL-4 intensity.

Competition assays

Antibody competition

4×10^4 cells were plated in 48-well plates. The cells were incubated with polyclonal goat antisera (8 µg/ml) against the Axl ectodomain or normal goat serum at 4 °C for 30 min. Pseudotyped VSV/EGFP/ΔG particles (MOI = 0.5) were added to the cells and the plate was shifted to 37 °C to promote transduction. Twenty h following transduction, the cells were lifted in Accumax (Fisher Scientific) and analyzed for EGFP expression using flow cytometry. The percentage of EGFP positive cells was compared to control cells transduced without antisera added.

Axl-Fc competition

VSV/EGFP/ΔG particles pseudotyped with either ZEBOV-GP ΔO or VSV-G were incubated with chimeric Axl ectodomain-Fc protein (Axl-Fc) (R&D Systems) (50 µg/ml) for 30 min at 4 °C. The mixture was transduced on to SNB-19 or 293T cells in a 48-well plate. Twenty-four h following transduction, cells were analyzed for EGFP expression using flow cytometry.

Generation of infectious, recombinant ZEBOV-GP ΔO VSV

A molecular clone of VSV containing EGFP in place of G that was generated by Dr. Jack Rose (Haglund et al., 2000) was kindly provided by Dr. Ira Bergman (University of Pittsburgh). The EGFP gene was inserted in place of VSV-G (Gao et al., 2006) and ZEBOV-GP ΔO was inserted upstream from EGFP. The construct along with plasmids expressing VSV N, P, M and L was transfected into BHK 21 cells as previously described (Haglund et al., 2000; Lawson et al., 1995). The full-length genome and each of the cDNAs were expressed from a T7 promoter sequence by infection of the cells with vTF7-3, a recombinant vaccinia virus expressing the T7 RNA polymerase. Supernatant was collected, filtered through a 0.2-µ filter and the virus was plaque purified. Immunoblotting of virus stocks verified expression of ZEBOV-GP. Stocks were titered by end point dilution on Vero cells.

Immunoblotting

Axl was detected using a goat polyclonal anti-Axl sera (0.2 µg/ml). Blots were washed and incubated with corresponding secondary HRP-conjugated sera.

AXL RNAi transfections

Two validated AXL RNAi constructs were purchased from Invitrogen along with an irrelevant control (Block-It). SNB-19 cells were transfected with 200 pmol of the RNAi using Lipofectamine 2000 (Invitrogen). Twenty-four h following transfection, the cells were lifted with trypsin and distributed into 48-well plates. For all RNAi knock-down experiments, cells were examined for Axl protein expression by immunoblotting and for Axl surface expression by flow cytometry at 48 h. We routinely observed a greater than 90% loss of Axl surface expression and a similar reduction in total Axl expression in cell lysates. In parallel, transfected cells that had been verified for Axl knock down were transduced with FIV particles bearing ZEBOV-GP ΔO FIV/β-galactosidase or VSV-G FIV/β-galactosidase and assayed for transduction as described above.

Transfection of cells with Axl expression plasmid

An expression plasmid bearing Axl was obtained from the Gene Transfer and Vector Core at the University of Iowa. NCI-H460 and NCI-H522 cells were transfected with 4 µg of the Axl expression plasmid or an equivalent empty plasmid using Lipofectamine 2000. Twenty-four h following transfection, the cells were lifted with trypsin and distributed into 48-well plates. Cells were examined for Axl surface expression by flow cytometry at 48 h. In parallel, transfected cells were transduced with ZEBOV-GP ΔO or VSV-G VSV pseudovirions and assayed for transduction by flow cytometry for EGFP expression as described above.

Virus internalization assay

SNB-19 cells seeded in a six-well plate at a concentration of 5×10^5 cells per well were transfected with 200 pmol of AXL RNAi (described above) or an irrelevant control RNAi (Block-It, Invitrogen) using Lipofectamine 2000. Twenty-four h after transfection, cells were lifted and replated in a 96-well plate at a concentration of 4×10^4 cells per well. The following day, 20 µl of media (containing 10% FBS, 1% P/S and ZEBOV-GP ΔO FIV or VSV-G FIV) were incubated with each well of cells for 1 h at 4 °C. After 1 h, media was removed and cells were washed once with 100 µl sterile PBS and 100 µl of pre-warmed media was added to each well for 1 h at 37 °C. At the termination of the experiment, media was removed. Cells were lifted and extracellular virus removed with a 5 min incubation with 100 µl of 0.25% trypsin/5 mM EDTA treatment. Trypsin/EDTA was neutralized with DMEM with FCS, and the cells were pelleted in a microcentrifuge for 4 min at 14,000 rpm. Supernatants were removed, and the pellet was lysed in 25 µl of sterile PBS containing 1% SDS. As a control, after the 4 °C incubation, cells were washed once and then lysed to determine the 100% value for total bound virions after 1 h. Cell lysates were kept at –20 °C until analysis by immunoblotting for β-actin or FIV capsid.

Immunoblot analysis of viral internalization assay

Proteins present in the cell lysates were separated on a 4–12% Bis-Tris NuPAGE gel (Invitrogen) and transferred onto nitrocellulose. FIV Capsid was detected by incubating with polyclonal anti-FIV antibody (1:5000) overnight at 4 °C and with secondary peroxidase-conjugated goat anti-feline antiserum (1:20,000; Amersham). β-actin was detected by incubating with a monoclonal anti-β-actin antibody conjugated to peroxidase (1:10,000) for 2 h at room temperature. Membranes were visualized using a Fujifilm Image Reader LAS-3000 (Fujifilm, Stamford, CT) and using the chemiluminescence method according to the manufacturer's protocol (Pierce). Data was analyzed and quantified using the Fujifilm Multi Gauge V2.3 program (Fujifilm, Stamford, CT). The capsid signal was normalized for actin levels and data are reported as the ratio of the FIV signal in the Axl knock down cells divided by the FIV signal in the cells transfected with an irrelevant RNA.

Viral transduction of AXL RNAi transfected cells with thermolysin-treated virus

SNB-19 cells were transfected with AXL RNAi as described above. Twenty-four h after transfection, cells were plated in a 48-well format at a concentration of 3.5×10^4 cells per well. FIV/β-gal pseudovirions bearing full-length ZEBOV-GP were treated for 5 min at 37 °C with 0.1 mg/ml of thermolysin (Sigma-Aldrich). Virus was then treated with 5 mM EDTA for 5 min at room temperature to neutralize the thermolysin. Thermolysin-treated or mock-treated virus was added to transfected cells at 48 h following transfection. Six h after the addition of thermolysin-treated virus, the virus was removed, media refreshed, and cells incubated for an additional 48 h at 37 °C. At the termination of the experiment, cells were fixed in PBS with 3.7%

formalin and evaluated for β -gal activity using the substrate 5-bromo-4-chloro-3-indolyl- β -D-galactopyranoside. The number of β -gal-positive cells was enumerated by microscopic visual inspection. The findings are shown as the number of transduced cells found in each treatment divided by the number of cells transduced by the untreated full-length ZEBOV-GP control. The numbers in parenthesis represent the effect of *AXL* RNAi treatment on transduction relative to the respective control.

Membrane fusion assay

SNB-19 cells were seeded at 3×10^4 cells per well in a 96-well plate and incubated with 20 μ g/ml (1:20) of goat anti-Axl antisera or normal goat sera for 1 h at 4 °C. Cells were shifted to 37 °C and incubated with 50 μ l of Src- β -lactamase containing ZEBOV-GP Δ O VLPs per well. After 12 h, VLPs within the media were removed and 0.1 mM CCF2-AM substrate was added to each well diluted in 100 μ l DMEM according to manufacturer's protocol (Invitrogen). Positive controls for the β -lactamase assay included pCMV-src- β -lactamase transfected and blue fluorescent protein (BFP) transfected cells. The plate was covered and incubated at room temperature for 2 h away from direct sunlight. After 2 h, the cells were trypsinized with 0.05% trypsin-EDTA (50 μ l per well) and resuspended in a total volume of 100 μ l (50 μ l trypsin + 50 μ l DMEM). Blue/green fluorescence was quantified in the cells using a three laser FACS Aria (Becton Dickinson) equipped with a 407 violet, a 488 blue, and a 633 red laser. Blue and green fluorescence was measured separately with emission filters 450/40 nm and 530/30 nm, respectively. The background blue fluorescence of untreated, CCF2-AM loaded control cells was subtracted as autofluorescence. Blue fluorescence was expressed as percentage blue cells in the population.

Confocal microscopy

SNB-19 cells (3.5×10^4 cells) were plated on collagen-coated coverslips and incubated overnight at 37 °C to allow cell adherence. Cells were incubated with ZEBOV-GP Δ O or VSV-G FIV pseudovirions (MOI = 250) at 4 °C for 1 h. Unbound virus was removed, cells were washed once in 1× PBS, and cells were shifted to 37 °C in pre-warmed media for the indicated times. At the indicated time, cells were fixed in 2% paraformaldehyde and not permeabilized or permeabilized with 0.2% Triton X-100. Virus (green) was detected with anti-FIV monoclonal antibody (1:50) and Alexa Fluor 488 chicken α -mouse (1:200; Invitrogen). Axl (red) was detected with anti-human Axl polyclonal antibody (1:150) and Alexa Fluor 568 donkey α -goat (1:200; Invitrogen). Microscopy was performed on a Nikon 801 confocal microscope with the gain set at the beginning of data collection and not subsequently changed.

Statistical analysis

Studies were performed at least three independent times except where noted in the figure legends. Means and standard errors of the mean are shown. Student's *t*-test was used to generate a *p* value to evaluate the statistical differences between treatments, utilizing the two-tailed distribution and two sample equal-variance conditions. Significance of the correlation findings in the NCI-60 screen was assessed by performing a linear correlation and regression and determining the *p* value from the two-tailed distribution. A significant difference was determined by a *p* value of <0.05 and level of significance was noted in each figure. If the *p* value was >0.05, the data were not considered statistically significantly different.

Supplementary materials related to this article can be found online at doi:10.1016/j.virol.2011.04.002.

Acknowledgments

This work was supported by NIHAI064526 and AI073330 (W.M.), NIHHL075363 (P.B.M.) and intramural NIH NIAID biodefense and NIH NIDCR grants to J.A.C. M.A.B. and A.S.K. were supported through NIHT32 A1007533, a training grant in molecular virology.

References

- Alvarez, C.P., Lasala, F., Carrillo, J., Muniz, O., Corbi, A.L., Delgado, R., 2002. C-type lectins DC-SIGN and L-SIGN mediate cellular entry by Ebola virus in cis and in trans. *J. Virol.* 76, 6841–6844.
- Barbaud, F., Doms, R.W., Pohlmann, S., 2002. The role of DC-SIGN and DC-SIGNR in HIV and Ebola virus infection: can potential therapeutics block virus transmission and dissemination? *Expert Opin. Ther. Targets* 6, 423–431.
- Bhattacharya, S., Warfield, K.L., Ruthel, G., Bavari, S., Aman, M.J., Hope, T.J., 2010. Ebola virus uses clathrin-mediated endocytosis as an entry pathway. *Virology* 401, 18–28.
- Braunger, J., Schleithoff, L., Schulz, A.S., Kessler, H., Lammers, R., Ullrich, A., Bartram, C.R., Janssen, J.W., 1997. Intracellular signaling of the Ufo/Axl receptor tyrosine kinase is mediated mainly by a multi-substrate docking-site. *Oncogene* 14, 2619–2631.
- Brindley, M.A., Hughes, L., Ruiz, A., McCray Jr., P.B., Sanchez, A., Sanders, D.A., Maury, W., 2007. Ebola virus glycoprotein 1: identification of residues important for binding and postbinding events. *J. Virol.* 81, 7702–7709.
- Budagian, V., Bulanova, E., Orinska, Z., Thon, L., Mammat, U., Bellostia, P., Basilico, C., Adam, D., Paus, R., Bulfone-Paus, S., 2005. A promiscuous liaison between IL-15 receptor and Axl receptor tyrosine kinase in cell death control. *EMBO J.* 24, 4260–4270.
- Cabreyer, N.B., Zhou, Y., Li, W., 2010. Tubby and tubby-like protein 1 are new MerTK ligands for phagocytosis. *EMBO J.* 29, 3898–3910.
- Carroll, K., Gomez, C., Shapiro, L., 2004. Tubby proteins: the plot thickens. *Nat. Rev. Mol. Cell Biol.* 5, 55–63.
- Cavrois, M., De Noronha, C., Greene, W.C., 2002. A sensitive and specific enzyme-based assay detecting HIV-1 virion fusion in primary T lymphocytes. *Nat. Biotechnol.* 20, 1151–1154.
- Cavrois, M., Neidleman, J., Bigos, M., Greene, W.C., 2004. Fluorescence resonance energy transfer-based HIV-1 virion fusion assay. *Methods Mol. Biol.* 263, 333–344.
- Chan, S.Y., Empig, C.J., Welte, F.J., Speck, R.F., Schmaljohn, A., Kreisberg, J.F., Goldsmith, M.A., 2001. Folate receptor-alpha is a cofactor for cellular entry by Marburg and Ebola viruses. *Cell* 106, 117–126.
- Chandran, K., Sullivan, N.J., Felbor, U., Whelan, S.P., Cunningham, J.M., 2005. Endosomal proteolysis of the Ebola virus glycoprotein is necessary for infection. *Science* 308, 1643–1645.
- Demarchi, F., Verardo, R., Varnum, B., Brancolini, C., Schneider, C., 2001. Gas6 anti-apoptotic signaling requires NF-kappa B activation. *J. Biol. Chem.* 276, 31738–31744.
- Di Pasquale, G., Davidson, B.L., Stein, C.S., Martins, I., Scudiero, D., Monks, A., Chiorini, J.A., 2003. Identification of PDGFR as a receptor for AAV-5 transduction. *Nat. Med.* 9, 1306–1312.
- Fridell, Y.W., Villa Jr., J., Attar, E.C., Liu, E.T., 1998. GAS6 induces Axl-mediated chemotaxis of vascular smooth muscle cells. *J. Biol. Chem.* 273, 7123–7126.
- Gao, Y., Whitaker-Dowling, P., Watkins, S.C., Griffen, J.A., Bergman, I., 2006. Rapid adaptation of a recombinant vesicular stomatitis virus to a targeted cell line. *J. Virol.* 80, 8603–8612.
- Geijtenbeek, T.B., van Kooyk, Y., 2003. Pathogens target DC-SIGN to influence their fate DC-SIGN functions as a pathogen receptor with broad specificity. *APMIS* 111, 698–714.
- Goruppi, S., Chiaruttini, C., Ruaro, M.E., Varnum, B., Schneider, C., 2001. Gas6 induces growth, beta-catenin stabilization, and T-cell factor transcriptional activation in contact-inhibited C57 mammary cells. *Mol. Cell. Biol.* 21, 902–915.
- Goruppi, S., Ruaro, E., Varnum, B., Schneider, C., 1997. Requirement of phosphatidylinositol 3-kinase-dependent pathway and Src for Gas6-Axl mitogenic and survival activities in NIH 3T3 fibroblasts. *Mol. Cell. Biol.* 17, 4442–4453.
- Goruppi, S., Ruaro, E., Varnum, B., Schneider, C., 1999. Gas6-mediated survival in NIH3T3 cells activates stress signalling cascade and is independent of Ras. *Oncogene* 18, 4224–4236.
- Hafizi, S., Gustafsson, A., Stenhoff, J., Dahlback, B., 2005. The Ran binding protein RanBP1 interacts with Axl and Sky receptor tyrosine kinases. *Int. J. Biochem. Cell Biol.* 37, 2344–2356.
- Haglund, K., Forman, J., Krausslich, H.G., Rose, J.K., 2000. Expression of human immunodeficiency virus type 1 Gag protein precursor and envelope proteins from a vesicular stomatitis virus recombinant: high-level production of virus-like particles containing HIV envelope. *Virology* 268, 112–121.
- Heiring, C., Dahlback, B., Muller, Y.A., 2004. Ligand recognition and homophilic interactions in Tyro3: structural insights into the Axl/Tyro3 receptor tyrosine kinase family. *J. Biol. Chem.* 279, 6952–6958.
- Hunt, C.L., Kolokoltsov, A.A., Davey, R.A., Maury, W., 2011. The Tyro3 receptor kinase Axl enhances macropinocytosis of Zaire ebolavirus. *J. Virol.* 85, 334–347.
- Jeffers, S.A., Sanders, D.A., Sanchez, A., 2002. Covalent modifications of the ebola virus glycoprotein. *J. Virol.* 76, 12463–12472.
- Lasala, F., Arce, E., Otero, J.R., Rojo, J., Delgado, R., 2003. Mannosyl glycodendritic structure inhibits DC-SIGN-mediated Ebola virus infection in cis and in trans. *Antimicrob. Agents Chemother.* 47, 3970–3972.
- Lawson, N.D., Stillman, E.A., Whitt, M.A., Rose, J.K., 1995. Recombinant vesicular stomatitis viruses from DNA. *Proc. Natl. Acad. Sci. USA* 92, 4477–4481.

- Lee, W.P., Liao, Y., Robinson, D., Kung, H.J., Liu, E.T., Hung, M.C., 1999. Axl-gas6 interaction counteracts E1A-mediated cell growth suppression and proapoptotic activity. *Mol. Cell. Biol.* 19, 8075–8082.
- Lin, G., Simmons, G., Pohlmann, S., Baribaud, F., Ni, H., Leslie, G.J., Haggarty, B.S., Bates, P., Weissman, D., Hoxie, J.A., Doms, R.W., 2003. Differential N-linked glycosylation of human immunodeficiency virus and Ebola virus envelope glycoproteins modulates interactions with DC-SIGN and DC-SIGNR. *J. Virol.* 77, 1337–1346.
- Linger, R.M., Keating, A.K., Earp, H.S., Graham, D.K., 2008. TAM receptor tyrosine kinases: biologic functions, signaling, and potential therapeutic targeting in human cancer. *Adv. Cancer Res.* 100, 35–83.
- Marzi, A., Gramberg, T., Simmons, G., Moller, P., Rennekamp, A.J., Krumbiegel, M., Geier, M., Eisemann, J., Turza, N., Saunier, B., Steinkasserer, A., Becker, S., Bates, P., Hofmann, H., Pohlmann, S., 2004. DC-SIGN and DC-SIGNR interact with the glycoprotein of Marburg virus and the S protein of severe acute respiratory syndrome coronavirus. *J. Virol.* 78, 12090–12095.
- McCloskey, P., Fridell, Y.W., Attar, E., Villa, J., Jin, Y., Varnum, B., Liu, E.T., 1997. GAS6 mediates adhesion of cells expressing the receptor tyrosine kinase Axl. *J. Biol. Chem.* 272, 23285–23291.
- Melaragno, M.G., Cavet, M.E., Yan, C., Tai, L.K., Jin, Z.G., Haendeler, J., Berk, B.C., 2004. Gas6 inhibits apoptosis in vascular smooth muscle: role of Axl kinase and Akt. *J. Mol. Cell. Cardiol.* 37, 881–887.
- Nielsen-Preiss, S.M., Allen, M.P., Xu, M., Linseman, D.A., Pawlowski, J.E., Bouchard, R.J., Varnum, B.C., Heidenreich, K.A., Wierman, M.E., 2007. Adhesion-related kinase induction of migration requires phosphatidylinositol-3-kinase and ras stimulation of rac activity in immortalized gonadotropin-releasing hormone neuronal cells. *Endocrinology* 148, 2806–2814.
- Quinn, K., Brindley, M.A., Weller, M.L., Kaludov, N., Kondratowicz, A., Hunt, C.L., Sinn, P.L., McCray Jr., P.B., Stein, C.S., Davidson, B.L., Flick, R., Mandell, R., Staplin, W., Maury, W., Chiorini, J.A., 2009. Rho GTPases modulate entry of Ebola virus and vesicular stomatitis virus pseudotyped vectors. *J. Virol.* 83, 10176–10186.
- Sasaki, T., Knyazev, P.G., Clout, N.J., Cheburkin, Y., Gohring, W., Ullrich, A., Timpl, R., Hohenester, E., 2006. Structural basis for Gas6-Axl signalling. *EMBO J.* 25, 80–87.
- Schornberg, K., Matsuyama, S., Kabsch, K., Delos, S., Bouton, A., White, J., 2006. Role of endosomal cathepsins in entry mediated by the Ebola virus glycoprotein. *J. Virol.* 80, 4174–4178.
- Scott, R.S., McMahon, E.J., Pop, S.M., Reap, E.A., Caricchio, R., Cohen, P.L., Earp, H.S., Matsushima, G.K., 2001. Phagocytosis and clearance of apoptotic cells is mediated by MER. *Nature* 411, 207–211.
- Shao, W.H., Zhen, Y., Eisenberg, R.A., Cohen, P.L., 2009. The Mer receptor tyrosine kinase is expressed on discrete macrophage subpopulations and mainly uses Gas6 as its ligand for uptake of apoptotic cells. *Clin. Immunol.* 133, 138–144.
- Shimojima, M., Ikeda, Y., Kawaoka, Y., 2007. The mechanism of Axl-mediated Ebola virus infection. *J. Infect. Dis.* 196 (Suppl 2), S259–S263.
- Shimojima, M., Takada, A., Ebihara, H., Neumann, G., Fujioka, K., Irimura, T., Jones, S., Feldmann, H., Kawaoka, Y., 2006. Tyro3 family-mediated cell entry of Ebola and Marburg viruses. *J. Virol.* 80, 10109–10116.
- Simmons, G., Reeves, J.D., Grogan, C.C., Vandenberghe, L.H., Baribaud, F., Whitbeck, J.C., Burke, E., Buchmeier, M.J., Soilleux, E.J., Riley, J.L., Doms, R.W., Bates, P., Pohlmann, S., 2003a. DC-SIGN and DC-SIGNR bind ebola glycoproteins and enhance infection of macrophages and endothelial cells. *Virology* 305, 115–123.
- Simmons, G., Rennekamp, A.J., Chai, N., Vandenberghe, L.H., Riley, J.L., Bates, P., 2003b. Folate receptor alpha and caveolae are not required for Ebola virus glycoprotein-mediated viral infection. *J. Virol.* 77, 13433–13438.
- Sinn, P.L., Hickey, M.A., Staber, P.D., Dylla, D.E., Jeffers, S.A., Davidson, B.L., Sanders, D.A., McCray Jr., P.B., 2003. Lentivirus vectors pseudotyped with filoviral envelope glycoproteins transduce airway epithelia from the apical surface independently of folate receptor alpha. *J. Virol.* 77, 5902–5910.
- Son, B.K., Kozaki, K., Iijima, K., Eto, M., Nakano, T., Akishita, M., Ouchi, Y., 2007. Gas6/Axl-PI3K/Akt pathway plays a central role in the effect of statins on inorganic phosphate-induced calcification of vascular smooth muscle cells. *Eur. J. Pharmacol.* 556, 1–8.
- Stitt, T.N., Conn, G., Gore, M., Lai, C., Bruno, J., Radziejewski, C., Mattsson, K., Fisher, J., Gies, D.R., Jones, P.F., et al., 1995. The anticoagulation factor protein S and its relative, Gas6, are ligands for the Tyro 3/Axl family of receptor tyrosine kinases. *Cell* 80, 661–670.
- Takada, A., Fujioka, K., Tsuji, M., Morikawa, A., Higashi, N., Ebihara, H., Kobasa, D., Feldmann, H., Irimura, T., Kawaoka, Y., 2004. Human macrophage C-type lectin specific for galactose and N-acetylgalactosamine promotes filovirus entry. *J. Virol.* 78, 2943–2947.
- Takada, A., Robison, C., Goto, H., Sanchez, A., Murti, K.G., Whitt, M.A., Kawaoka, Y., 1997. A system for functional analysis of Ebola virus glycoprotein. *Proc. Natl. Acad. Sci. USA* 94, 14764–14769.
- Varnum, B.C., Young, C., Elliott, G., Garcia, A., Bartley, T.D., Fridell, Y.W., Hunt, R.W., Trail, G., Clogston, C., Toso, R.J., et al., 1995. Axl receptor tyrosine kinase stimulated by the vitamin K-dependent protein encoded by growth-arrest-specific gene 6. *Nature* 373, 623–626.
- Weinger, J.G., Gohari, P., Yan, Y., Backer, J.M., Varnum, B., Shafit-Zagardo, B., 2008. In brain, Axl recruits Grb2 and the p85 regulatory subunit of PI3 kinase; in vitro mutagenesis defines the requisite binding sites for downstream Akt activation. *J. Neurochem.* 106, 134–146.
- Weller, M.L., Amorphimoltham, P., Schmidt, M., Wilson, P.A., Gutkind, J.S., Chiorini, J.A., 2010. Epidermal growth factor receptor is a co-receptor for adeno-associated virus serotype 6. *Nat. Med.* 16, 662–664.
- Wilhelm, I., Nagyoszi, P., Farkas, A.E., Couraud, P.O., Romero, I.A., Weksler, B., Fazakas, C., Dung, N.T., Bottka, S., Bauer, H., Bauer, H.C., Krizbai, I.A., 2008. Hyperosmotic stress induces Axl activation and cleavage in cerebral endothelial cells. *J. Neurochem.* 107, 116–126.
- Wool-Lewis, R.J., Bates, P., 1998. Characterization of Ebola virus entry by using pseudotyped viruses: identification of receptor-deficient cell lines. *J. Virol.* 72, 3155–3160.
- Zhang, Y.X., Knyazev, P.G., Cheburkin, Y.V., Sharma, K., Knyazev, Y.P., Orfi, L., Szabadkai, I., Daub, H., Keri, G., Ullrich, A., 2008. AXL is a potential target for therapeutic intervention in breast cancer progression. *Cancer Res.* 68, 1905–1915.
- Zheng, Y., Zhang, L., Lu, Q., Wang, X., Yu, F., Wang, X., Lu, Q., 2009. NGF-induced Tyro3 and Axl function as survival factors for differentiating PC12 cells. *Biochem. Biophys. Res. Commun.* 378, 371–375.